Article

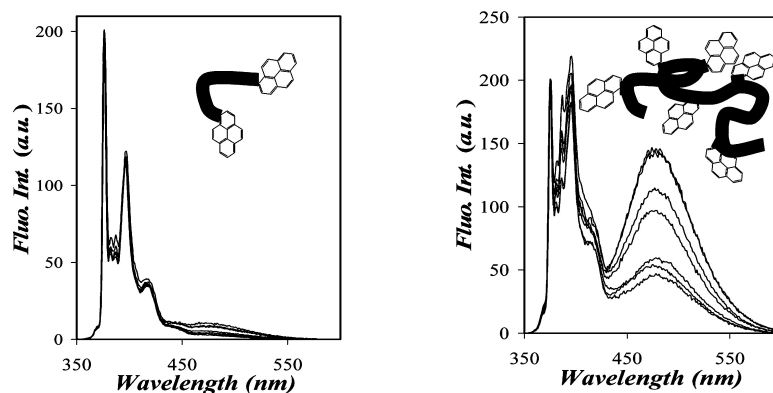# A Case for Using Randomly Labeled Polymers to Study Long-Range Polymer Chain Dynamics by Fluorescence

Mark Ingratta, Jon Hollinger, and Jean Duhamel

More About This Article

Additional resources and features associated with this article are available within the HTML version:

- Supporting Information
- Links to the 1 articles that cite this article, as of the time of this article download
- Access to high resolution figures
- Links to articles and content related to this article
- Copyright permission to reproduce figures and/or text from this article

View the Full Text HTML

ACS Publications
High quality. High impact.

A Case for Using Randomly Labeled Polymers to Study Long-Range Polymer Chain Dynamics by Fluorescence

Mark Ingratta, Jon Hollinger, and Jean Duhamel*

Institute for Polymer Research, Department of Chemistry, University of Waterloo, 200 University Avenue West, Waterloo Ontario N2L 3G1, Canada

Received February 4, 2008; E-mail: jduhamel@uwaterloo.ca

Abstract: The process of excimer formation was studied for a series of pyrene end-labeled polystyrenes (PS(*X*)-Py₂ where *X* is the polymer molecular weight equal to 3, 4.5, 8, 12.7, and 14.6 K) and two series of polystyrenes randomly labeled with pyrene (CoE-PS and CoA-PS) in seven different solvents. The solvent viscosities ranged from 0.41 to 1.92 mPa·s, while the solvent quality ranged from good to poor solvents for polystyrene, as determined by intrinsic viscosity measurements. Steady-state fluorescence spectra of the pyrene-labeled polymers were acquired, and the excimer to monomer ratios showed that excimer formation increased strongly with a decrease in solvent viscosity. The monomer and excimer time-resolved fluorescence decays were also acquired and fitted globally to either the Birks' scheme or the fluorescence blob model (FBM) for the end- or randomly labeled polymers, respectively. All parameters reporting on the long-range polymer chain dynamics (LRPCD) obtained from the analysis of the fluorescence data acquired with the PS(*X*)-Py₂, CoE-PS, and CoA-PS series yielded virtually identical trends, demonstrating that these fluorescence experiments yield results that are internally consistent with one another. Considering the substantial advantages associated with the preparation and study of randomly labeled polymers, this report presents an appealing case for the use of randomly labeled polymers in the study of LRPCD.

Introduction

The relatively recent realization[1] that time-resolved fluorescence and phosphorescence techniques were particularly well-suited to deliver valuable information on the time scale over which the most basic step in protein folding occurs, namely loop formation, has triggered an outburst of research that uses triplet−triplet energy transfer (TTET),[2–8] fluorescence resonance energy transfer (FRET),[9] or fluorescence dynamic quenching (FDQ)[10–13] to measure the rate of end-to-end cyclization (EEC) of short peptides (*N* < 50 amino acids) labeled at both ends with appropriate chromophores. These experiments are based on the same principle, namely covalently attaching at one end of the chain one chromophore that interacts with another

chromophore covalently attached at the other end of the chain and monitoring the time scale over which these interactions take place during an EEC event. They take advantage of a long-standing scientific interest in EEC[14–19] that led to the conclusion that EEC events can be described by a single rate constant, an important simplification considering the complex photochemical processes often encountered when dealing with TTET, FRET, or FDQ experiments.[2–13]

The use of TTET, FRET, and FDQ to study peptide chain dynamics has been reviewed in detail and critically compared recently.[10] The phosphorescent chromophore/quencher pairs (xanthone/naphthalene,[3,6–8] diphenylketone/naphthalene,[4] or tryptophan/cystein[5]) have been used in TTET experiments, and energy transfer between the phosphorescent chromophores and their quencher occurs via a Dexter mechanism over distances which, as argued recently,[10] are short but, strictly speaking, larger than the contact encounter radius of the chromophore

(1) Eaton, W. A.; Muñoz, V.; Hagen, S. J.; Jas, G. S.; Lapidus, L. J.; Henry, E. R.; Hofrichter, J. *Annu. Rev. Biophys. Biomol. Struct.* **2000**, *29*, 327–359.
(2) Hagen, S. J.; Hofrichter, J.; Szabo, A.; Eaton, W. A. *Proc. Natl. Acad. Sci. U.S.A.* **1996**, *93*, 11615–11617.
(3) Bieri, O.; Wirz, J.; Hellrung, B.; Schutkowski, M.; Drewello, M.; Kiefhaber, T. *Proc. Natl. Acad. Sci. U.S.A.* **1999**, *96*, 9597–9601.
(4) McGimpsey, W. G.; Chen, L.; Carraway, R.; Samaniego, W. N. *J. Phys. Chem. A* **1999**, *103*, 6082–6090.
(5) Lapidus, L. J.; Eaton, W. A.; Hofrichter, J. *Proc. Natl. Acad. Sci. U.S.A.* **2000**, *97*, 7220–7225.
(6) Krieger, F.; Fierz, B.; Bieri, O.; Drewello, M.; Kiefhaber, T. *J. Mol. Biol.* **2003**, *332*, 265–274.
(7) Möglich, A.; Krieger, F.; Kiefhaber, T. *J. Mol. Biol.* **2005**, *345*, 153–162.
(8) Fierz, B.; Satzger, H.; Root, C.; Gich, P.; Zinth, W.; Kiefhaber, T. *Proc. Natl. Acad. Sci. U.S.A.* **2007**, *104*, 2163–2168.
(9) Möglich, A.; Joder, K.; Kiefhaber, T. *Proc. Natl. Acad. Sci. U.S.A.* **2006**, *103*, 12394–12399.
(10) Hudgins, R. R.; Huang, F.; Gramlich, G.; Nau, W. M. *J. Am. Chem. Soc.* **2002**, *124*, 556–564.
(11) Huang, F.; Hudgins, R. R.; Nau, W. M. *J. Am. Chem. Soc.* **2004**, *126*, 16665–16675.
(12) Roccatano, D.; Sahoo, H.; Zacharias, M.; Nau, W. M. *J. Phys. Chem. B* **2007**, *111*, 2639–2646.
(13) Neuweiler, H.; Löllmann, M.; Doose, S.; Sauer, M. *J. Mol. Biol.* **2007**, *365*, 856–869.
(14) Flory, P. J.; Suter, U. W.; Mutter, M. *J. Am. Chem. Soc.* **1976**, *98*, 5733–5739.
(15) Wilemski, G.; Fixman, M. *J. Chem. Phys.* **1974**, *60*, 866–877.
(16) Wilemski, G.; Fixman, M. *J. Chem. Phys.* **1974**, *60*, 878–890.
(17) Szabo, A.; Schulten, K.; Schulten, Z. *J. Chem. Phys.* **1980**, *72*, 4350–4357.
(18) Winnik, M. A. *Chem. Rev.* **1981**, *81*, 491–524.
(19) Cuniberti, C.; Perico, A. *Prog. Polym. Sci.* **1984**, *10*, 271–316.

and quencher.[20] FRET experiments have been carried out by monitoring the energy transfer from an excited dansyl to a ground-state pyrene attached at a peptide ends.[9] FRET occurs via a Förster mechanism over large distances, usually much larger than the contact encounter radius of the donor and acceptor pair.[21] This feature complicates somewhat the analysis of the fluorescence data since the distribution of the chain ends needs to be accounted for. Out of all three techniques, FDQ has the unique advantage of occurring upon direct contact of the fluorophore and its quencher. The diazabicyclooctene/ tryptophan[10–12] or oxazine/tryptophan[13] pairs attached at opposite ends of a peptide have been used as fluorophore/quencher pairs.

Regardless of the technique, studies on EEC are inherently limited by the strong dependency of the rate constant of EEC (k_{cy}) with polymer chain length (N). As a matter of fact, k_{cy} is theoretically expected[15–17,19] and experimentally found[22,23] to scale as $N^{-\gamma}$ where γ equals 1.5 (1.6 in the case of ref 22) when the polymer diffuses in the solution as a nondraining chain. This dependency implies that a 10-fold increase in chain length reduces k_{cy} by no less than 97%! In other words, increasing the chain length of a polymer drastically decreases the very number of EEC events necessary to measure the chain dynamics of the end-labeled chain. The magnitude of this detrimental effect is well-documented when k_{cy} is measured by FDQ experiments monitoring the rate constant of excimer formation for pyrene end-labeled polystyrenes.[24] In that case, k_{cy} cannot be measured directly from time-resolved fluorescence measurements for polystyrene chains longer than 100 units. Whereas this effect is a nonissue for the shorter peptides of current interest, it will inescapably become one as the long-range polymer chain dynamics (LRPCD) of more realistic protein mimics are investigated such as those encountered in longer polypeptides.

The solution to this problem is obviously trivial. If end-labeling of the chain keeps the chromophores too far apart to yield enough EEC events, the chromophores should be brought closer to one another by incorporating them into the chain at either regular or random intervals along the chain. Reducing the chain length spanning two chromophores enhances the rate of internal cyclization, generating more events that reflect the long-range polymer chain dynamics (LRPCD) of the macromolecules. Unfortunately, time-resolved FDQ experiments have shown that, for both cases, chromophore encounters are described, not by a single rate constant as is the case for EEC experiments,[15–17,19,22] but by a distribution of rate constants when chromophores are incorporated at multiple internal positions along the chain.[25,26] This distribution of rate constants arises from the spatial distribution of the labels inside the polymer coil as well as from the distribution of chain lengths spanning every two labels randomly attached along the backbone. These complications have prevented any quantitative information on polymer chain dynamics to be obtained directly from time-resolved fluorescence measurements until 1999 when

this laboratory established that the distribution of rate constants resulting from these different labeling arrangements can be handled satisfyingly by a fluorescence blob model (FBM).[27,28]

The FBM functions by compartmentalizing the polymer coil into blobs where a blob represents the volume equivalent to that probed by the excited chromophore during its natural lifetime. The quenchers distribute themselves randomly into the blobs according to a Poisson distribution, and the kinetics of encounters between the excited chromophore and the quenchers are handled using the same mathematical treatment used when dealing with chromophores and quenchers randomly distributed among surfactant micelles.[29,30] The many advantages associated with using the FBM have been reviewed recently.[28] Among them is the ability of the FBM to handle polydisperse polymers since a long or short polymer simply requires the use of more or less identical blobs, respectively. In other words, the focus of a FBM study is being shifted from the entire polymer chain as is being done for EEC to that chain segment making up a blob. Furthermore, the FBM retrieves quantitative information on LRPCD from polymers labeled randomly or at specific internal positions of the chain.[31] Finally, the FBM works with chromophore/quencher pairs that specifically undergo FDQ such as in the case of pyrene excimer formation. Quenching or excimer formation occurs upon contact between two chromophores, a definite advantage to monitor LRPCD.

This report compares the results obtained on LRPCD from the analysis of fluorescence data acquired with two series of polystyrenes randomly labeled with pyrene, the CoA-PS and CoE-PS series, and a series of five pyrene end-labeled monodisperse polystyrenes (PS(X)-Py$_2$) of molecular weight $X = 3.0$, 4.5, 8.0, 12.7, and 14.6 K. The CoA-PS and CoE-PS series were obtained by copolymerizing styrene with either 1-pyrenemethylacrylamide or 4-(1-pyrenyl)methoxymethylstyrene, respectively.[31] The pyrene monomer and excimer fluorescence decays of the CoA-PS and CoE-PS polymers were analyzed with the FBM,[28] whereas those of the PS(X)-Py$_2$ were analyzed with the Birks' scheme.[32] These experiments were carried out in seven organic solvents of quality toward polystyrene ranging from poor to good and with viscosities between 0.41 and 1.92 mPa.s. Comparison of the results obtained with the randomly and end-labeled polymers demonstrated unambiguously the momentous enhancement in excimer formation resulting from the random labeling of the chain. Since excimer formation is the process by which information on LRPCD is gained, generating more excimer simplifies drastically the study of LRPCD. More importantly, it was also found that, within experimental error and regardless of solvent quality, solvent viscosity, or polystyrene series, the parameters describing LRPCD obtained via the FBM analysis with the randomly labeled polymers or the Birks' scheme analysis with the end-labeled polymers yielded virtually identical trends, demonstrating that the exact same information on LRPCD can be retrieved for a given polymer regardless of the manner used to incorporate the labels into the chain.

The momentous enhancement in signal enabled by the random labeling of polymers is expected to open new venues of research

(20) Grätzel, M. *Heterogeneous Photochemical Electron Transfer*; CRC Press: Boca Raton, 1989.
(21) Förster, T. *Z. Naturforsch., A: Phys. Sci.* **1949**, *4*, 321–327.
(22) Winnik, M. A. *Acc. Chem. Res.* **1985**, *18*, 73–79.
(23) Zachariasse, K. A.; Maçanita, A. L.; Kühnle, W. *J. Phys. Chem. B* **1999**, *103*, 9356–9365.
(24) Winnik, M. A.; Redpath, A. E. C.; Paton, K.; Danhelka, J. *Polymer* **1984**, *25*, 91–99.
(25) Winnik, M. A.; Li, X.-B.; Guillet, J. E. *Macromolecules* **1984**, *17*, 699–702.
(26) Winnik, M. A.; Egan, L. S.; Tencer, M.; Croucher, M. D. *Polymer* **1987**, *28*, 1553–1560.

(27) Mathew, A.; Siu, H.; Duhamel, J. *Macromolecules* **1999**, *32*, 7100–7108.
(28) Duhamel, J. *Acc. Chem. Res.* **2006**, *39*, 953–960.
(29) Tachiya, M. *Chem. Phys. Lett.* **1975**, *33*, 289–292.
(30) Infelta, P. P.; Graetzel, M.; Thomas, J. K. *J. Phys. Chem.* **1974**, *78*, 190–195.
(31) Ingratta, M.; Duhamel, J. *Macromolecules* **2007**, *40*, 6647–6657.
(32) Birks, J. B. *Photophysics of Aromatic Molecules*. Wiley: New York, 1970; p 301.

Table 1. Pyrene Contents x in mol % (see Scheme 1) and λ_{Py} in μmol g^{-1}, Molecular Weights and PDI of the PS(X)–Py$_2$, CoA-PS and CoE-PS Samples.

sample	x, mol % Py	λ_{Py}, μmol·g^{-1}	M_n, kg·mol^{-1}	PDI
CoE-PS	1.5	141	35	1.81
	1.8	169	45	1.87
	3.2	284	32	1.99
	4.8	412	16	1.85
	5.1	436	34	1.80
	6.4	533	46	1.65
CoA-PS	1.1	105	43	1.88
	2.5	230	39	2.04
	3.7	331	55	1.90
	5.0	437	28	1.88
	5.2	459	34	1.96
	6.4	550	39	1.91
PS(X)–Py$_2$	1.4	137	14.6	1.10
	1.6	157	12.7	1.20
	2.6	250	8.0	1.09
	4.6	444	4.5	1.12
	6.9	667	3.0	1.10

toward the study of the LRPCD of longer and stiffer backbones, such as those of proteins. Although it could be objected that the random incorporation of fluorescent labels into a polypeptide of well-defined sequence might not be as easily accomplished as the specific incorporation of two different chromophores at the amino- and carboxy-ends of a short peptide,[2–13] it must be noted that model polypeptides have already been randomly labeled with pyrene.[33] In particular, the FBM has been applied to monitor the side-chain dynamics of pyrene-labeled poly(L-glutamic acid).[34]

Experimental Section

Materials. Distilled in glass N,N-dimethylformamide (DMF), tetrahydrofuran (THF), and dioxane were purchased from Caledon Laboratories (Georgetown, ON). Certified ACS methyl ethyl ketone (MEK) was purchased from Fischer Scientific (Fair Lawn, NJ). HPLC grade dichloromethane (DCM) and toluene were purchased from EMD Science (Gibbstown, NJ). HPLC grade N,N-dimethylacetamide (DMA) was purchased from Sigma-Aldrich (Oakville, ON). All solvents were used as received. The α,ω-dicarboxyl end-capped polystyrenes were purchased from Polymer Source (Montréal, QC). 4-(1-Pyrene)-butylamine hydrochloride was purchased from Toronto Research Chemicals.

Synthesis of the Polystyrenes Randomly Labeled with Pyrene. The synthesis and characterization of poly(styrene-co-1-pyrenemethylacrylamide) (CoA-PS) and poly(styrene-co-4-(1-pyrenyl)-methoxymethyl styrene) (CoE-PS) have been described in a previous article.[31] The pyrene content expressed in mol% of pyrene labeled monomer (x) or μmol of pyrene per gram of polymer (λ_{Py}), the number-average molecular weight, and the polydispersity index of the Py-PS samples are listed in Table 1. The number average molecular weights of the Py-PSs were typically ~40 kg/mol with a PDI of ~1.9. The structures of the PS(X)-Py$_2$, CoA-PS, and CoE-PS polymers are shown in Scheme 1.

(33) Shoji, O.; Ohkawa, M.; Kuwata, H.; Sumida, T.; Kato, R.; Annaka, M.; Yoshikuni, M.; Nakahira, T. *Macromolecules* **2001**, *34*, 4270–4276.

(34) Duhamel, J.; Kanagalingam, S.; O'Brien, T.; Ingratta, M. *J. Am. Chem. Soc.* **2003**, *125*, 12810–12822.

(35) James, D. R.; Demmer, D. R.; Verall, R. E.; Steer, R. P. *Rev. Sci. Instrum.* **1983**, *54*, 1121–1130.

Synthesis of the Pyrene End-Labeled Polystyrenes. The PS(X)-Py$_2$ samples, namely PS(3)-Py$_2$, PS(4.5)-Py$_2$, PS(8)-Py$_2$, PS(12.7)-Py$_2$, and PS(14.6)-Py$_2$, were prepared by reacting α,ω-dicarboxyl end-capped polystyrene having M_n equal to, respectively, 3.0, 4.5, 8.0, 12.7, and 14.6 K with 4-(1-pyrene)-butylamine hydrochloride. An example synthesis is described for the polymer having an M_n of 4.5 kg/mol.

In a 7 mL vial, 100 mg (0.022 mmol) 4500 g/mol α,ω-dicarboxyl end-capped polystyrene, 135 mg (0.44 mmol) 4-(1-pyrene)butylamine hydrochloride, 8.4 mg (0.044 mmol) EDC, 5.8 mg (0.044 mmol) HOBt, 0.50 g (0.05 mmol) triethylamine, and 1.5 mL DMF were added. The reaction was stirred at room temperature for 20 h. The polymer was precipitated in methanol, redissolved in THF, and precipitated in methanol 5−7 times to remove unreacted 4-(1-pyrene)butylamine. After their synthesis and purification, the labeled polymers were characterized by size exclusion chromatography (SEC) and UV−vis absorption. SEC was performed to ensure all unreacted pyrene derivatives were removed. SEC was carried out using a Waters system with THF as the eluent and a Jordi linear DVB mixed-bed column. The instrument was coupled with a fluorescence detector with excitation and emission wavelengths set at 344 and 375 nm, respectively. Sample concentrations were ~3 mg/mL. No unreacted pyrene derivative was found to elute with the solvent peak in the SEC traces, confirming that all pyrene present in the sample was bound to the polymer. The pyrene content, as determined in the following section using UV−vis spectroscopy, led to the conclusion that the labeling reaction achieved ~80% yield, indicating that singly labeled polymers are present in the mixture and will fluoresce with the natural lifetime of the pyrene monomer, τ_M. The singly labeled chains act as an impurity in the decays of the mostly doubly labeled chains. However, their detrimental effect is reduced by the fact that singly labeled chains absorb twice less excitation photons than doubly labeled chains. Furthermore, this unwanted emission is accounted for in the global analysis of the time-resolved fluorescence decays and is not detrimental to the Birks analysis.[32] The analysis is discussed in greater detail in the Analysis of the Fluorescence Decays section.

Pyrene Content Determination. A Hewlett-Packard 8452A diode array spectrophotometer was used for the absorption measurements. The pyrene content of the polymer (λ_{Py}) is obtained by dissolving a known mass of pyrene labeled polymer (m) in a known volume of DMF (V). The concentration of pyrene, [Py], is then determined by applying Beer−Lambert's Law to the peak absorption at 344 nm and using the extinction coefficients (ε_{Py}) of the model compounds 1-pyrenebutyric acid, 4-(1-pyrene)butylamide, and 4-(1-pyrene)butylamine for PS(X)-Py$_2$ in DMF or 1-pyrenemethylacrylamide and 1-pyrenemethanol for CoA-PS and CoE-PS in DMF. The three pyrenebutyl- and two pyrenemethyl-derivatives yielded similar ε_{Py} values equal to 37,200 ± 1,000 M^{-1}·cm^{-1} and 39,000 ± 1,000 M^{-1}·cm^{-1}, respectively. The pyrene content, λ_{Py}, whose expression is given in eq 1, is expressed in μmole of pyrene per gram of polymer (μmol·g^{-1}).
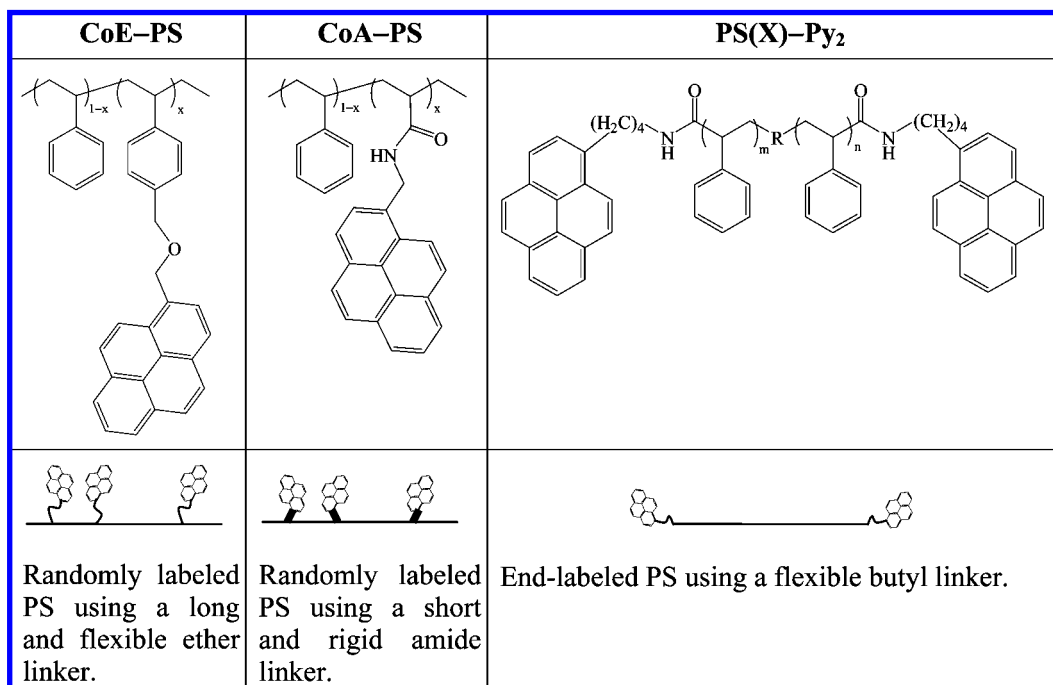
$$\lambda_{Py} = \frac{[Py]}{m/V} \qquad (1)$$

For the PS(X)-Py$_2$ series, λ_{Py} is calculated by considering the fully labeled chains only, i.e. for a PS chain with a molecular weight of 4500 g/mol, λ_{Py} equals 2/4500 = 440 μmol·g^{-1}. The pyrene content of all pyrene-labeled polymers is listed in Table 1.

Scheme 1. Chemical Structures of CoA-PS, CoE-PS and PS(*X*)–Py₂

Table 2. Solvent Viscosities, Intrinsic Viscosities, and Qualities for PS-40K at $T = 25\ °C$.

solvent	η, mPa·s	$[\eta]_{40K}$, L/g	$\pm[\eta]$, L/g	quality
methyl ethyl ketone (MEK)	0.41	0.0178	0.0002	poor
dichloromethane (DCM)	0.41	0.0248	0.0004	good
tetrahydrofuran (THF)	0.46	0.0246	0.0014	good
toluene	0.56	0.0259	0.0003	good
N,N-dimethylformamide (DMF)	0.79	0.0192	0.0003	poor
dioxane	1.18	0.0241	0.0001	good
N,N-dimethylacetamide (DMA)	1.92	0.0221	0.0007	mediocre

Intrinsic Viscosity Measurements. A narrow molecular weight polystyrene (PS-40K, $M_n = 40$ kg/mol; $M_w = 42$ kg/mol) was used as a model for the CoA-PS and CoE-PS series. The pyrene-labeled polymers were not used themselves due to the very small amount of pyrene-labeled polymer synthesized (typically ~40 mg). Four to five concentrations ranging from 3 to 10 g/L were used to find the intrinsic viscosities for PS in each solvent. The viscosity measurements were conducted with an Übbelohde viscometer placed in an ethylene glycol bath maintained at a temperature of $25 \pm 0.1\ °C$. Plots of the reduced viscosity as a function of the polymer concentration are shown in Figure SI.1 in Supporting Information (SI). The intrinsic viscosity ($[\eta]$) of PS-40K in different solvents was obtained by extrapolating the plots shown in Figure SI.1 to zero polymer concentration. The $[\eta]$ values are reported in Table 2.

Steady-State Fluorescence Measurements. All fluorescence spectra were obtained on a PTI fluorometer using the right angle geometry. All solutions had an optical density of 0.1 and were degassed for 30 min under a gentle flow of N₂ to remove oxygen. The degassed solutions were excited at 344 nm, and the emission spectrum was collected from 350 to 600 nm. The fluorescence intensity of the monomer (I_M) and excimer (I_E) was integrated between 372 and 378 nm and between 500 and 530 nm, respectively.

Time-Resolved Fluorescence Measurements. Fluorescence decays were obtained by exciting the solutions at 340 nm with

Scheme 2. Birks' Scheme for the Formation of Excimer with a Pyrene End-Labeled Monodisperse Polymer[22,32]
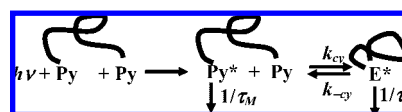
an IBH 340 nm LED and collecting the emission at 375 and 510 nm for the monomer and excimer, respectively. All decays were acquired using 1024 channels to a peak maximum of 20,000 counts for the lamp and decay curves. The instrument response function was determined by applying the MIMIC method[35] to the reference decays obtained with PPO [2,5-diphenyloxazole] in cyclohexanol ($\tau = 1.42$ ns) and BBOT [2,5-bis(*tert*-butyl-2-benzoxazolyl)thiopene] in ethanol ($\tau = 1.47$ ns) for the monomer and excimer decays, respectively. The polymer solutions were prepared in the same manner as for the steady-state fluorescence experiments.

Analysis of the Fluorescence Decays. The monomer and excimer decays of PS(*X*)-Py₂ were fit globally and according to the Birks' Scheme (Scheme 2).[22,32] The Birks' Scheme dictates that the monomer and excimer fluorescence decays be biexponential, and that the same decay times be obtained in both decays. One complication encountered when dealing with pyrene end-labeled polymers has to do with the impossibility of getting fully double-labeled chains. The polymers supplied by Polymer Source contain a small amount of monofunctionalized chains, and the labeling reaction is not 100% efficient. Thus, a small amount of chains labeled at one end with pyrene are always present in the mixture. Since the monolabeled chains emit as the pyrene monomer with a lifetime τ_M, they can be easily accounted for by adding a third exponential to the monomer decays. The sums of exponentials used to fit the monomer and excimer decays globally are given in eqs 2 and 3.

$$I_M(t) = a_{M1} \exp(-t/\tau_1) + a_{M2} \exp(-t/\tau_2) + a_M \exp(-t/\tau_M)$$
(2)

$$I_M(t) = a_{E1} \exp(-t/\tau_1) + a_{E1} \exp(-t/\tau_2)$$
(3)

Table 3. Pyrene Monomer Lifetimes, τ_M, Retrieved from Low Pyrene-Labeled PS Samples.

solvent	CoE-PS, τ_M (ns)	CoA-PS, τ_M (ns)	PS(8)–Py, τ_M (ns)
methyl ethyl ketone	172	170	117
dichloromethane	144	152	105
tetrahydrofuran	257	258	190
toluene	230	241	172
N,N-dimethylformamide	220	220	160
dioxane	242	243	175
N,N-dimethylacetamide	215	215	160

The lifetime of the unquenched pyrene monomer was determined through the analysis of the fluorescence decays of a low pyrene content polymer (PS(X)-Py) obtained by reacting the α,ω-dicarboxyl end-capped polystyrene with a small amount of 1-pyrenebutylamine to ensure that a majority of the chains were labeled with pyrene at one end only. The τ_M values obtained with PS(X)-Py for a particular polymer–solvent system range from 105 to 190 ns for PS(X)-Py$_2$ (Table 3). After fitting the monomer and excimer decays globally with eqs 2 and 3, the rate constants k_{cy}, k_{-cy}, and $1/\tau_E$ in Scheme 2 are determined from the parameters a_{M1}/a_{M2}, τ_1, and τ_2 following the well-established procedure described by Birks.[22,32] All parameters obtained from the fits and kinetic rate constants are listed in Tables SI.1 and SI.2.

The monomer and excimer decays of CoA-PS and CoE-PS were analyzed globally with the FBM whereby the monomer and excimer decays were simultaneously fitted with eqs 4 and 5, respectively.[36]

$$[\text{Py*}]_{(t)} = [\text{Py}^*_{\text{diff}}]_{(t=0)} \exp\left[-\left(A_2 + \frac{1}{\tau_M}\right)t - A_3(1 - \exp(-A_4 t))\right] + [\text{Py}^*_{\text{free}}]_{(t=0)} \exp(-t/\tau_M) \quad (4)$$

$$[\text{E*}] = -[\text{Py}^*_{\text{diff}}]_{(t=0)} \exp[-A_3] \times$$

$$\sum_{i=0}^{\infty} \frac{A_3^i}{i!} \frac{A_2 + iA_4}{\frac{1}{\tau_M} - \frac{1}{\tau_{E0}} + A_2 + iA_4} \times \exp\left(-\left(\frac{1}{\tau_M} + A_2 + iA_4\right)t\right) +$$

$$\left([\text{E0*}]_{(t=0)} + [\text{Py}^*_{\text{diff}}]_{(t=0)} \exp[-A_3] \times \right.$$

$$\left. \sum_{i=0}^{\infty} \frac{A_3^i}{i!} \frac{A_2 + iA_4}{\frac{1}{\tau_M} - \frac{1}{\tau_{E0}} + A_2 + iA_4}\right) + \exp(-t/\tau_{E0}) +$$

$$[\text{D*}]_0 \exp(-t/\tau_D) \quad (5)$$

The parameters A_2, A_3, and A_4 used in eqs 1 and 2 are described in eq 6. Equations 4–6 have been used extensively over the past decade to study polymer chain dynamics in solution.[28]

$$A_2 = \langle n \rangle \frac{k_{\text{blob}} k_e[\text{blob}]}{k_{\text{blob}} + k_e[\text{blob}]} A_3 = \langle n \rangle \frac{k_{\text{blob}}^2}{(k_{\text{blob}} + k_e[\text{blob}])^2}$$

$$A_4 = k_{\text{blob}} + k_e[\text{blob}] \quad (6)$$

Equations 4–6 assume that some of the excimer is formed through diffusive encounters between an excited pyrene, Py$^*_{\text{diff}}$, and a ground-state pyrene. In the monomer decay, the Py$^*_{\text{diff}}$ monomers are described by the first exponential in eq 4. The

fraction of pyrene groups that are isolated and cannot form excimer, Py$^*_{\text{free}}$, are accounted for by the second exponential in eq 4. The lifetime of the unquenched pyrene monomer, τ_M, was estimated through the biexponential analysis of the fluorescence decays of a low pyrene content CoE-PS and CoA-PS sample (<0.2 mol % pyrene) where the exponential with the longest decay time contributed more than 80% of the total pre-exponential weight of the decay. The lifetimes were found to be in the 144−258 ns range, depending on the solvent as shown in Table 3. It must be noted that the 1-pyrenemethyl chromophore has a ∼50 ns larger lifetime than the 1-pyrenebutyl chromophore. The FBM parameters retrieved from the analysis of the monomer decay and used in eq 4 are defined as the rate constant of encounter between one excited pyrene and one ground-state pyrene located in the same blob, k_{blob}, the average number of ground-state pyrenes per blob, $\langle n \rangle$, and the rate constant describing the exchange of ground-state pyrenes between blobs times the blob concentration in the polymer coil, $k_e \times [\text{blob}]$.

Equation 5 fits the excimer decays assuming three pathways toward excimer formation. The excimers, E0*, formed through the diffusive encounter of an excited pyrene, Py$^*_{\text{diff}}$, and a ground-state pyrene emit with a lifetime τ_{E0}. They can also be generated through direct excitation of a preassociated dimer, E0. The long-lived pyrene dimers, D*, fluoresce with a long lifetime τ_D resulting from improper stacking of the two pyrene moieties. The extremely small contribution of D* to the excimer decays in organic solvents (<0.05 in Tables SI.5 and SI.8) makes it impossible to determine τ_D accurately. It was found that a τ_D value of 180 ns would yield excellent fits regardless of pyrene content. Consequently, τ_D was fixed to this value in the global analysis of all the fluorescence decays obtained with CoA-PS and CoE-PS. The simultaneous analysis of the monomer and excimer decays enables the determination of the fractions f_{diff}, f_{free}, f_{E0}, and f_D of the species Py$^*_{\text{diff}}$, Py$^*_{\text{free}}$, E0*, D* and the sum of the fractions $f_{E0} + f_D$ gives the fraction of aggregated pyrene groups, f_{agg}. Determination of these species is described in more detail in a previous publication.[37]

Optimization of the parameters used in eqs 4–6 to fit globally the monomer and excimer fluorescence decays was performed with the Marquardt−Levenberg algorithm.[38] The IBH 340 LED laser used to acquire the fluorescence decays was found to generate a higher background noise level than the hydrogen lamp used previously. Therefore a background correction was applied to fit the fluorescence decays.[39] As done in earlier publications, a light-scattering correction was also applied to account for those pyrene pairs which are in close contact and form excimer on a time scale which is too fast to be detected accurately by our instrument.[40] The fits of the monomer and excimer decays were considered good if the χ^2 was below 1.3 and the residuals were randomly distributed around zero.

Results and Discussion

The kinetics of intrachain pyrene−pyrene encounters were studied in several organic solvents, namely MEK, DCM, THF,

(36) Siu, H.; Duhamel, J. *Macromolecules* **2004**, *37*, 9287–9289.

(37) Prazeres, T. J. V.; Beingessner, R.; Duhamel, J.; Olesen, K.; Shay, G.; Bassett, D. R. *Macromolecules* **2001**, *34*, 7876–7884.
(38) Press, W. H.; Flannery, B. P.; Teukolsky, S. A.; Vetterling, W. T. *Numerical Recipes. The Art of Scientific Computing (Fortran Version)*; Cambridge University Press: Cambridge, 1992.
(39) Demas, J. N. *Excited-State Lifetime Measurements*; Academic Press: New York, 1983.
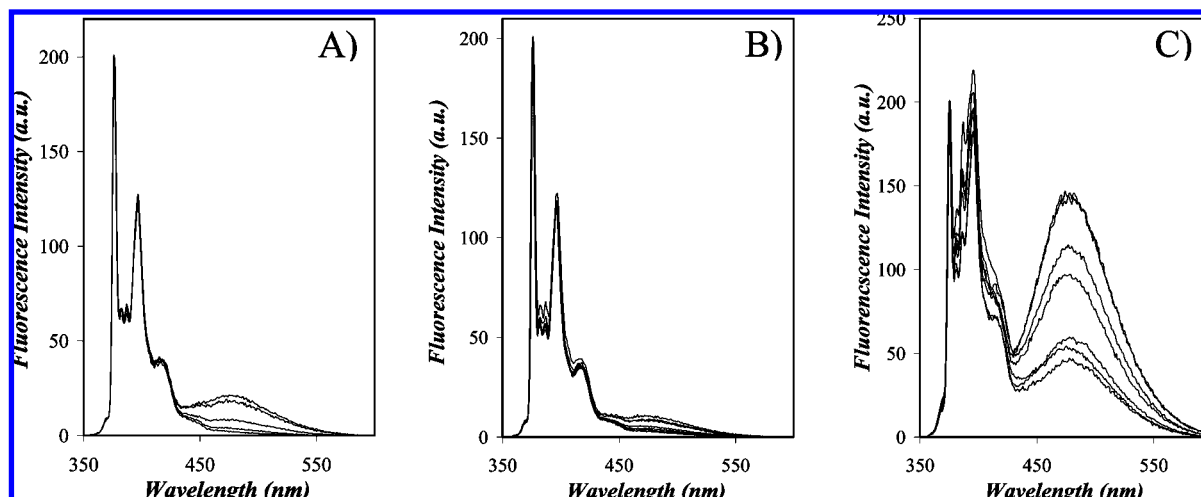(40) Martinho, J. M. G.; Egan, L. S.; Winnik, M. A. *Anal. Chem.* **1987**, *59*, 861–864.

Figure 1. Steady-state fluorescence spectra of polystyrene labeled with pyrene (A) PS(X)-Py$_2$ in toluene with, from top to bottom, X = 3.0, 4.5, 8.0, 12.7, 14.6; (B) PS(8)-Py$_2$ (x = 2.6 mol %) in, from top to bottom, MEK, DCM, THF, toluene, DMF, dioxane, and DMA; and (C) CoE-PS (x = 1.8 mol %) in the same organic solvents as in B). [Py] = 3×10^{-6} M, λ_{ex} = 344 nm.

toluene, DMF, dioxane, and DMA, that were chosen to provide a broad range of viscosities (0.41 − 1.92 mPa·s). The quality of the solvents toward PS was assessed from intrinsic viscosity measurements. Intrinsic viscosity measurements were conducted at 25 °C for each of the solvents using the PS-40K sample, a monodisperse PS with an M_n of 40 kg/mol and M_w of 42 kg/mol. The plots relating the specific viscosity of the polymer solutions to the polymer concentration are shown in Figure SI.1. THF, toluene, dioxane, and DCM being known good solvents for PS at 25 °C[41] yield large and similar [η] values for PS-40K, confirming that the quality of these solvents toward PS is good, whereas MEK, DMF, and DMA yielding lower [η] values are poorer solvents. The intrinsic viscosities obtained for PS-40K in THF, toluene, and MEK are in good agreement with the intrinsic viscosities of a PS sample having an M_w of 42 kg/mol calculated with the published Mark−Houwink−Sakurada (MHS) constants in their respective solvents.[41] All [η] values are listed in Table 2, together with the solvent quality toward polystyrene estimated from [η].

Steady-state fluorescence spectra were acquired for five PS(X)-Py$_2$, six CoA-PS, and six CoE-PS samples in seven organic solvents, and several of these spectra are shown in Figures 1A−C. Figure 1A which shows the fluorescence spectra of all five PS(X)-Py$_2$ samples in toluene demonstrates the dramatic effect that increasing polymer chain length has on the generation of excimer: the further apart the pyrenes are kept and the more hindered excimer formation is. Figures 1B for the PS(8)-Py$_2$ sample and 1C for the CoE-PS sample with a pyrene content of 1.8 mol % illustrate the effect that increasing the viscosity has on excimer formation. Comparison of Figure 1B with Figure 1C leads to two observations. First and as expected, increased viscosity reduces pyrene−pyrene encounters, resulting in a strong reduction in excimer formation for both samples. Second, the fluorescence spectra shown in parts B and C of Figure 1 vividly illustrate that EEC events occur much less frequently than intrachain encounters.

All effects shown in spectra A−C of Figure 1 are readily rationalized by using the theoretical framework developed by Wilemski and Fixman[15,16] and applied by Cuniberti and Perico[19]

to estimate a theoretical expression of the ratio of the fluorescence intensity of the excimer over that of the monomer, the I_E/I_M ratio. At temperatures smaller than 30 °C, the rate constant for excimer dissociation is usually neglected with respect to $1/\tau_E$ and the I_E/I_M ratio is given by eq 7[42]

$$\frac{I_E}{I_M} = \kappa \frac{\phi_E^o}{\phi_M^o} \tau_M k_1 [Py]_{loc} \qquad (7)$$

where κ is a constant that depends on the geometry and sensitivity of the spectrofluorometer used, k_1 is the bimolecular encounter rate constant which for free pyrenes would equal $2 \times RT/(3 \times \eta)$ with R, T, and η being respectively the ideal gas constant, the absolute temperature in K, and the solvent viscosity, ϕ_M^o and ϕ_E^o are the fluorescence quantum yields of, respectively, the pyrene monomer and excimer, τ_M is the natural lifetime of the pyrene monomer, and $[Py]_{loc}$ represents the effective concentration of the unexcited chromophores in the neighborhood of the excited species. Differences in the behavior expected for randomly labeled or end-labeled chain stem mostly from $[Py]_{loc}$ whose theoretical expression has been reported.[19,42]

Equation 7 provides a solid theoretical basis to explain qualitatively the trends observed in panels A−C of Figure 1. An increase in chain length for end-labeled polymers decreases $[Py]_{loc}$ which results in a decrease of the I_E/I_M ratio as found experimentally in Figure 1A and predicted by eq 7. Through k_1, eq 7 also predicts that I_E/I_M is inversely proportional to the solvent viscosity. This is also observed experimentally in panels B and C of Figure 1 for an end-labeled and a randomly labeled polystyrene, respectively. The most important observation to be made about panels B and C of Figure 1 is the outstanding enhancement in excimer formation observed for the randomly labeled sample. Whereas an end-labeled monodisperse polymer holds the pyrenes at a well-defined distance, the randomly labeled polymer enables pyrene pairs to be separated by shorter polymer stretches which generate excimer with a much larger rate constant and in a much higher yield. Those nearby located pyrenes form pyrene-rich domains inside the polymer coil that absorb a larger fraction of the excitation photons and contribute more strongly to excimer formation. Consequently, $[Py]_{loc}$ is

(41) Bandrup, J.; Immergut, E. H.; Grulke, E. A. *Polymer Handbook*, 4th ed.; John Wiley & Sons: New York, 1999, Vol. VII, pp 675−683.

(42) Cuniberti, C.; Perico, A. *Eur. Polym. J.* **1980**, *16*, 887–893.
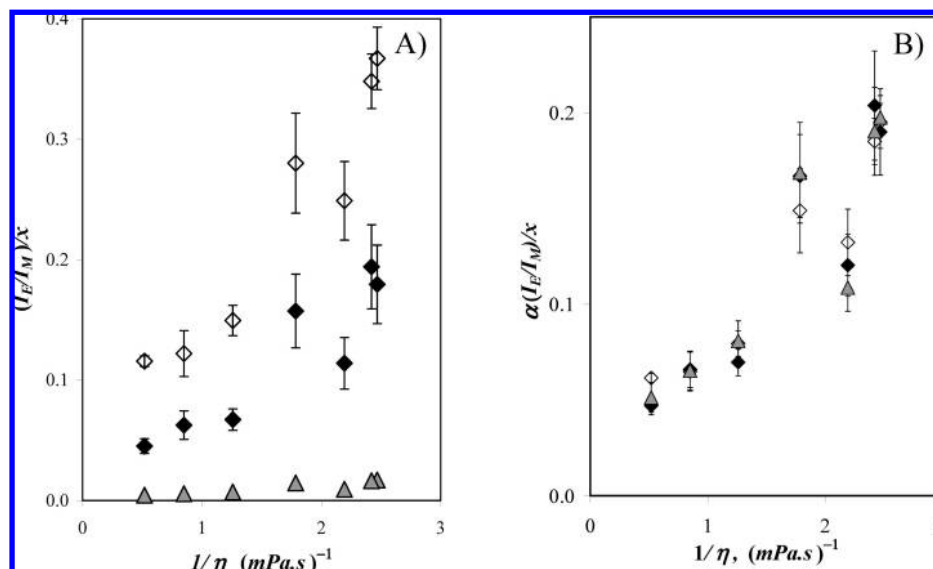
Figure 2. (A) $(I_E/I_M)/x$ and (B) $\alpha \times (I_E/I_M)/x$ as a function of $1/\eta$ for PS(8)–Py$_2$ (gray filled traingles); CoE-PS ($\diamond$); and CoA-PS ($\blacklozenge$) where $\alpha = 10.8, 0.49$, and 1.0, respectively.

larger for the randomly labeled polymers resulting in the substantial enhancement of the I_E/I_M ratio found when comparing Figure 1B with Figure 1C.

The results shown in Figure 1 and rationalized qualitatively through the use of eq 7 bring two important points to the fore: (1) Regardless of solvent viscosity or quality, excimer formation occurs much more efficiently with the randomly labeled polymer rather than the end-labeled polymer. (2) The much weaker excimer fluorescence intensity of PS(8)-Py$_2$ makes it very difficult to study end-labeled polymers made of a longer PS chain, as illustrated by Figure 1A. This complication does not occur with randomly labeled polymers since intramolecular excimer formation for a randomly labeled polymer describes a local phenomenon which occurs with the same frequency regardless of chain length as was found experimentally.[27,28] From these two points, the two following conclusions can be drawn: (1) The LRPCD of long polymer chains such as those encountered in typical proteins can not be studied easily by the end-to-end cyclization approach. (2) The spectra obtained with CoE-PS in Figure 1C suggest that information on LRPCD should be accessible from the response of long chains randomly labeled with a chromophore.

The I_E/I_M ratios were measured for the 17 polymer samples in seven different solvents yielding 119 data points. In an effort to condense the amount of information, the I_E/I_M ratios were divided by the molar fraction of labeled monomer in the polymer (x) to account for [Py]$_{loc}$. However, the longer PS(12.7)-Py$_2$ and PS(14.6)-Py$_2$ polymers which were found to generate too little excimer for accurate determination of the Birks' scheme parameters (*vide infra*) and the CoA-PS and CoE-PS samples that had too large a fraction of pyrene monomers that did not form excimer ($f_{free} > 0.10$ in Tables SI.5 and SI.8 for x smaller than 1.5 mol %) were not used. Within experimental error, the quantities $(I_E/I_M)/x$ merged into a single value. The observations made in B and C of Figure 1 about the efficiency of excimer formation are reproduced in Figure 2A where $(I_E/I_M)/x$ is plotted as a function of $1/\eta$. $(I_E/I_M)/x$ for the end-labeled polymers is much smaller than that of the randomly labeled polymers regardless of solvent viscosity or quality.

The bimolecular rate constant of excimer formation, k_1 in eq 7, is known to depend on the nature of the linker connecting

pyrene to the polymer. For instance, CoA-PS where pyrene is connected to the backbone via a short and stiff amide linker has been shown to have a k_1 value that is half-that of CoE-PS where pyrene is connected to the backbone via a longer and more flexible ether linker.[31] Also, k_1 must be larger with the unhindered end-labeled polymers than with the randomly labeled ones. Furthermore, the fluorescence quantum yields of the pyrene monomer (ϕ_M^o) and excimer (ϕ_E^o) and the monomer lifetime (τ_M) generated by the three polymer series are expected to be different, depending on the polymer series. The parameters ϕ_M, ϕ_E^o, τ_M, and k_1 affect the I_E/I_M ratio according to eq 7. Although these differences due to the chemical nature of the different linkers connecting pyrene to the PS backbone are difficult to account for exactly, they appear to affect $(I_E/I_M)/x$ for a given polymer series in the same manner regardless of polymer series or solvent. By multiplying $(I_E/I_M)/x$ by the factor α equal to 10.8, 0.49, and 1.0 for, respectively, the PS(X)-Py$_2$, CoE-PS, and CoA-PS series yield trends that are virtually identical. This result suggests that as long as [Py]$_{loc}$ is accounted for by dividing the I_E/I_M ratio by x as was done for the polymers selected in this study, the quantity $\alpha \times (I_E/I_M)/x$ yields information about k_1, and this information is the same whether it is obtained with a pyrene end-labeled or randomly labeled polystyrene. In other words, information on LRPCD obtained from pyrene-labeled polymers depends uniquely on the polystyrene backbone and not on the nature of the labeling, an expected but usually never proven result. Another observation made from A and B of Figure 2 is the expected overall increase of $\alpha \times (I_E/I_M)/x$ with $1/\eta$ which reflects the increased mobility of the pyrene monomers and is predicted by eq 7.

Time-resolved fluorescence decay measurements were conducted to confirm the promising results obtained by steady-state fluorescence, namely that the same information on LRPCD can be obtained with pyrene labeled polymers, regardless of the labeling procedure. The monomer and excimer decays of the five PS(X)-Py$_2$, six CoA-PS, and six CoE-PS samples were acquired in the seven solvents. The results obtained from the analysis of the fluorescence decays of the PS(X)-Py$_2$ samples are discussed first. The monomer and excimer decays were fitted globally with eqs 2 and 3, respectively. The fits were excellent with residuals and autocorrelation of the residuals randomly
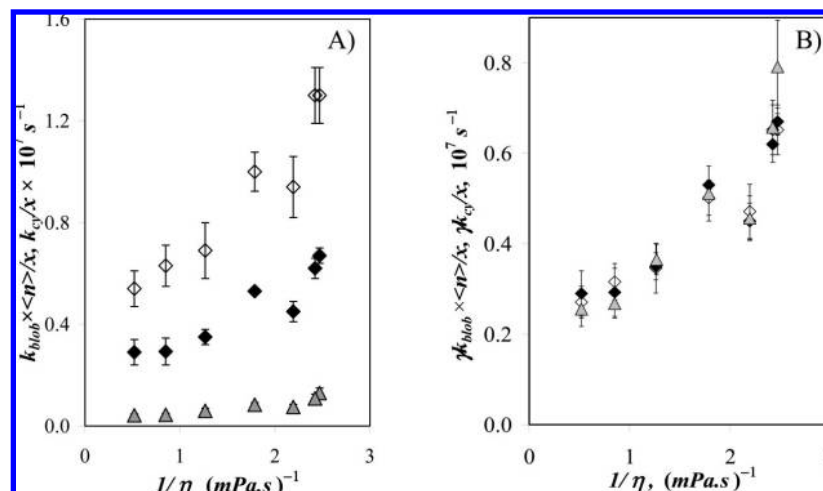
Figure 3. (A) $k_{blob} \times \langle n \rangle / x$ or k_{cy}/x and (B) $\gamma \times k_{blob} \times \langle n \rangle / x$ or $\gamma \times k_{cy}/x$ as a function of $1/\eta$ for PS(8)–Py$_2$ (gray filled traingles); CoE-PS ($\diamond$); and CoA-PS ($\blacklozenge$) where $\gamma = 6.1$, 0.50, and 1.0, respectively.

distributed around zero and χ^2 smaller than 1.30. The pre-exponential factors and decaytimes retrieved from the analysis are listed in Table SI.1. The parameters k_{cy}, k_{-cy}, and τ_E in Scheme 2 were obtained from the decaytimes τ_1 and τ_2 and the ratio a_{M2}/a_{M1} according to the procedure outlined by Birks.[32] On the one hand, the results obtained with the three shorter polymers followed the expected trends. In each solvent, k_{cy} decreases with increasing chain length since a longer chain keeps the pyrenes apart and hinders EEC;[22] τ_E remains constant around 54 ± 4 ns, as often found for the pyrene excimer in organic solvents;[24,32] and k_{-cy} takes a small value around $3 \times 10^6 \pm 1 \times 10^6$ s^{-1}.[24] On the other hand, the parameters retrieved from the analysis of the fluorescence decays obtained with PS(12.7)-Py$_2$ and PS(14.6)-Py$_2$ are suspect. First, τ_E for the PS(12.7)-Py$_2$ sample is much larger than 55 ns in all solvents but MEK. This is not possible because τ_E is an intrinsic property of the excimer that is not supposed to change with chain length. Second, the ratio of the pre-exponential factors a_{E1}/a_{E2} equals -0.80 for PS(14.7)-Py$_2$ instead of the value of -0.95 ± 0.02 obtained for the shorter polymers. Ideally, an a_{E1}/a_{E2} ratio equal to -1.0 would be obtained if excimer formation was occurring via diffusive encounters only. This condition is obeyed for the shorter polymers but not for PS(14.6)-Py$_2$. The reasons behind the discrepancies obtained for PS(12.7)-Py$_2$ and PS(14.6)-Py$_2$ are well-known for scientists versed in the trade of analyzing complex multiexponential fluorescence decays. For PS(12.7)-Py$_2$, the discrepancy is due to the sharp decrease of k_{cy} with increasing chain length which becomes too small with respect to τ_M^{-1} to be retrieved with accuracy. In the case of PS(14.6)-Py$_2$, k_{cy} is actually so small that not enough excimer is generated and the monomer fluorescence leaks into the excimer decays. These results are consistent with the conclusion drawn almost 25 years ago that the straightforward Birks' analysis of the monomer and excimer fluorescence decays can not be carried out for PS(X)-Py$_2$ samples where X is greater than 10.[24] Consequently, only the data obtained with the three shorter polymers were considered, as was done earlier with the I_E/I_M ratios.

The pseudounimolecular rate constant k_{cy} for excimer formation with the PS(X)-Py$_2$ polymers is the product of a bimolecular rate constant k_1^{cy} for diffusion-controlled end-to-end encounters times $[Py]_{loc}$.[19] The superscript "cy" for k_1^{cy} refers to the diffusion experienced by the flexible chain ends which occurs more

rapidly than the diffusion experienced by internal segments of the chain. In turn, $[Py]_{loc}$ for EEC experiments represents the local concentration of a single ground-state pyrene in the polymer coil. As done with the I_E/I_M ratio, k_{cy} was divided by the mole fraction of pyrene labeled monomers x to account for changes in $[Py]_{loc}$ due to changes in chain lenth. All k_{cy}/x ratios yielded similar values whose average was plotted as a function of $1/\eta$ in Figure 3A. As expected for a diffusion-controlled reaction, k_{cy}/x increases with $1/\eta$ reflecting the enhanced mobility experienced by the chromophores as the viscosity decreases.[43]

The monomer and excimer decays of the CoA-PS and CoE-PS series were acquired and fitted globally according to the FBM with eqs 4 and 5, respectively. The fits were good, and the parameters retrieved from the fits have been listed in Tables SI.3−8. The fraction of pyrenes that were close to one another, a result of the random incorporation of the label, was found to be small and between 10 and 20 mol % in the vast majority of cases (see Tables SI.5 and SI.8 for the results obtained with CoE-PS and CoA-PS). This result confirms that excimer formation for CoE-PS and CoA-PS occurs mostly via diffusion-controlled encounters between pyrene pendants that are not clustered but randomly distributed along the chain, and that excimer formation reflects the LRPCD of the chain.[31]

Within the FBM framework, k_{blob} is a pseudo-unimolecular rate constant describing the rate of excimer formation by diffusion between an excited pyrene and a ground-state pyrene, both located in the same blob.[28,44] Consequently, k_{blob} is the product of the bimolecular rate constant k_1^{blob}, where the superscript "blob" indicates that intrachain segmental encounters are considered, times the local concentration equivalent to one ground-state pyrene inside a blob, namely $k_{blob} = k_1^{blob} \times (1/V_{blob})$. Consequently, multiplying k_{blob} by $\langle n \rangle$ yields eq 8.

$$k_{blob} \times \langle n \rangle = k_1^{blob} \times \frac{\langle n \rangle}{V_{blob}} = k_1^{blob} \times [Py]_{loc} \quad (8)$$

The product $k_{blob} \times \langle n \rangle$ was divided by x for all CoA-PS and CoE-PS samples to account for the increase in $[Py]_{loc}$ resulting from an increase in pyrene content. A single $k_{blob} \times \langle n \rangle / x$ value

(43) Cheung, S.-T.; Winnik, M. A.; Redpath, A. E. C. *Makromol. Chem.* **1982**, *183*, 1815–1824.

(44) Kanagalingam, S.; Spartalis, J.; Cao, T.-C.; Duhamel, J. *Macromolecules* **2002**, *35*, 8571–8577.

was obtained for a given polymer series in a given solvent. The averaged $k_{blob} \times \langle n \rangle /x$ values were plotted as a function of $1/\eta$ in Figure 3A for the CoA-PS and CoE-PS series. The quantity $k_{blob} \times \langle n \rangle /x$ was found to increase with $1/\eta$ reflecting the fact that excimer formation is a diffusion-controlled process. Also, the inherently larger $[Py]_{loc}$ obtained for randomly labeled polymers is clearly illustrated in Figure 3A where k_{cy}/x takes values which are much smaller than $k_{blob} \times \langle n \rangle /x$. This trend is internally consistent with that shown in Figure 2A for the I_E/I_M ratios.

As was done for the I_E/I_M ratios, the k_{cy}/x and $k_{blob} \times \langle n \rangle /x$ trends obtained in seven different solvents were multiplied by a constant scaling factor γ that equaled 6.1, 0.50, and 1.0 for the PS(*X*)-Py$_2$, CoE-PS, and CoA-PS series, respectively. The values of $\gamma \times k_{cy}/x$ for the PS(*X*)-Py$_2$ series and $\gamma \times k_{blob} \times \langle n \rangle /x$ for the CoE-PS and CoA-PS series were plotted as a function of $1/\eta$ in Figure 3B. Both Figures 2B and 3B yield trends that are virtually identical for the end-labeled and the randomly labeled polymers. This result leads to a rather important conclusion, namely that the kinetic information contained in the fluorescence responses of PS(*X*)-Py$_2$, CoE-PS, and CoA-PS are, strictly speaking, the same. In other words, the same information on the LRPCD of a polymer can be attained either from the k_{cy} value retrieved from the Birks' Scheme analysis of the fluorescence decays acquired with a monodisperse polymer terminated at both ends with two pyrenes, or from the $k_{blob} \times \langle n \rangle$ product retrieved from the FBM analysis of the fluorescence decays acquired with a polydisperse polymer randomly labeled with pyrene.

Considering that (1) polydisperse polymers randomly labeled with a chromophore are usually much easier to prepare than monodisperse polymers labeled at both ends with a chromophore, (2) intramolecular encounters between chromophores randomly distributed along a chain occur much more frequently than end-to-end cyclization events, (3) polymers of any chain length can be studied when they are randomly labeled with a chromophore, and (4) analysis of the fluorescence decays acquired with the FBM yields kinetic information identical to that obtained with a pyrene end-labeled monodisperse polymer, the present study implies that LRPCD can be studied much more easily and efficiently with randomly labeled polymers rather than end-labeled polymers. These conclusions are expected to impact profoundly those fields of research interested in characterizing the LRPCD of macromolecules by spectroscopic means, as for the study of protein folding[1-13] or the rheological behavior of polymer solutions.[45]

Conclusions

The LRPCD of polystyrene was investigated by steady-state and time-resolved fluorescence using polymers that were labeled with the chromophore pyrene in three different manners. A series of five monodisperse polystyrenes were end-labeled with pyrene, yielding the PS(*X*)-Py$_2$ series. These polymers were found to yield little excimer, and the little amount of excimer generated

(45) Siu, H.; Duhamel, J. *Macromolecules* **2006**, *39*, 1144–1155.

was found to decrease rapidly with increasing chain length, making it impossible to retrieve any reliable information on the rate constant of excimer formation (k_{cy}) from time-resolved fluorescence experiments for polymer samples having an M_n larger than 10,000 g·mol^{-1}. The k_{cy} rate constants for the PS(*X*)-Py$_2$ samples having $X < 10$ were obtained from the global analysis of the monomer and excimer fluorescence decays conducted according to the Birks scheme. Similar k_{cy}/x values were obtained for all three PS(*X*)-Py$_2$ samples having an M_n value smaller than 10,000 g·mol^{-1}, and the averaged k_{cy}/x value was found to increase with $1/\eta$, as expected for excimer formation controlled by solvent viscosity.

Two series of six polydisperse polystyrenes were prepared by random copolymerization of styrene with a pyrene-labeled monomer yielding the CoA-PS and CoE-PS series. The monomer and excimer fluorescence decays were acquired for all samples and were analyzed globally according to the FBM. In any given solvent, $k_{blob} \times \langle n \rangle /x$ remained constant with pyrene content. The quantities k_{cy}/x and $k_{blob} \times \langle n \rangle /x$ were found to yield similar trends increasing with $1/\eta$, confirming that fluorescence experiments conducted on pyrene-labeled polystyrenes yield the same information on the LRPCD of polystyrene, regardless of how the polymer is being labeled.

The gain in signal resulting from using randomly labeled polymers together with the FBM analysis to retrieve quantitative information on LRPCD makes an appealing case for using randomly labeled polymers in the study of LRPCD and opens new venues of research to study much slower LRPCD such as those encountered with stiffer polymers, at lower temperature, or in higher viscosity solvents. The LRPCD of long chains, which are presently inaccessible to classical EEC experiments, can now be studied experimentally via time-resolved fluorescence measurements. In particular, this study opens a path toward characterizing the LRPCD encountered in long and stiff polypeptides which can be viewed as protein mimics. The use of randomly labeled polymers is expected to complement advantageously the rich arsenal of photophysical techniques used presently to study short peptides by EEC processes.[2-13]

Supporting Information Available: Figure SI.1, plot of reduced viscosity versus polymer concentration in different organic solvents; Figure SI.2, fits of the monomer and excimer fluorescence decays for CoE-PS in DMF; Figure SI.3, fits of the monomer and excimer fluorescence decays for CoA-PS in DMF; Figure SI.4, plots of f_{agg} versus the corrected pyrene content for CoA-PS (A) and CoE-PS (B) in different organic solvents; Tables SI.1−8, parameters retrieved from the fit of the fluorescence decays using eqs 2–6. This material is available free of charge via the Internet at http://pubs.acs.org.

JA800897M